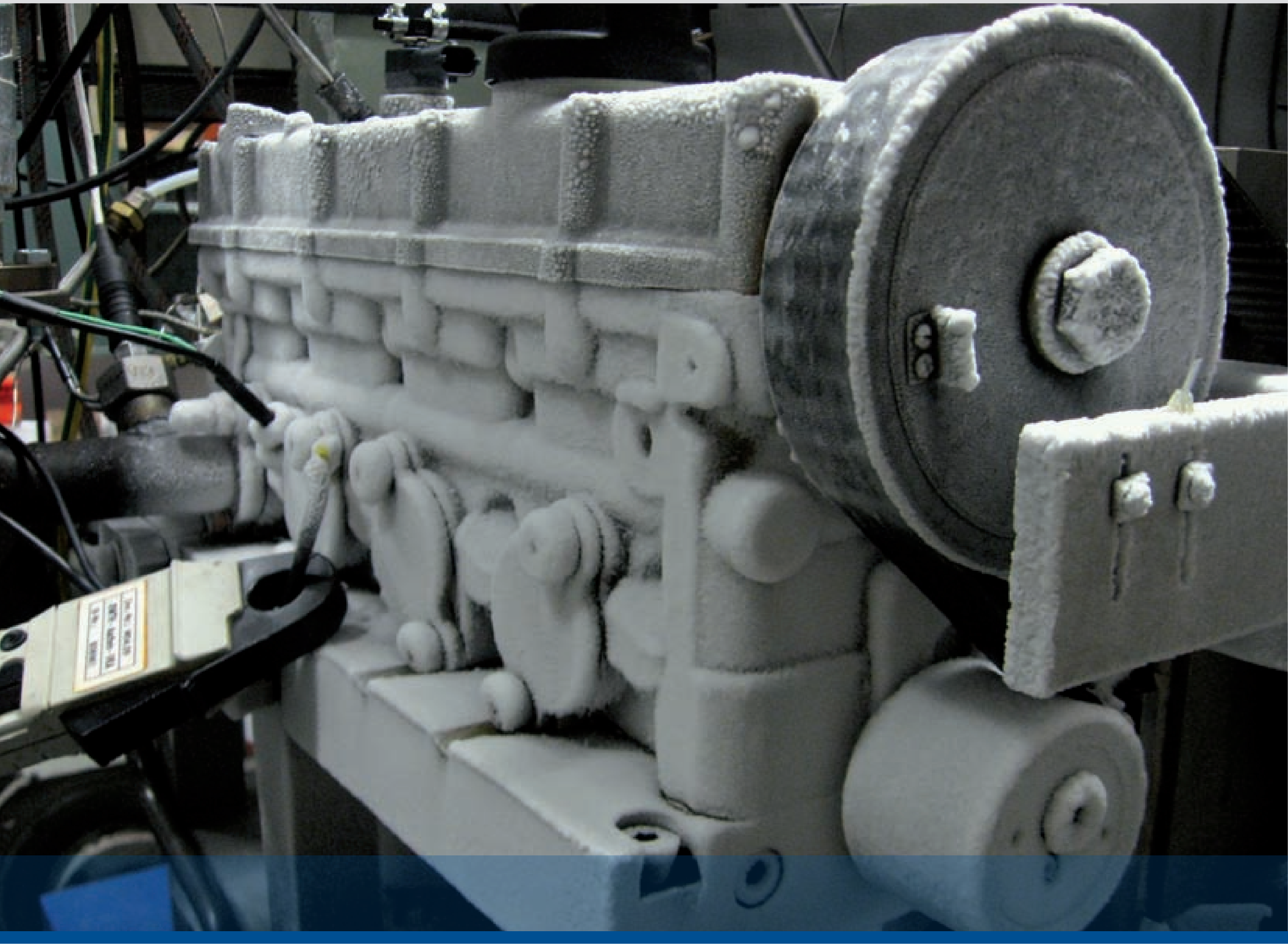

# Ignition of Diesel Fuel at Low Temperatures

As part of a research project funded by the Research Association for Combustion Engines (FVV), fundamental research on the ignition of diesel fuel at low temperatures was undertaken at the Institute for Combustion Engines (VKA) of RWTH Aachen University. The motivation for this project is the fact that new diesel engine generations have the tendency towards lower compression. One the one hand, combustion processes have the high potential to significantly reduce exhaust raw emissions, one the other hand, lower final compression pressures and temperatures aggravate the self ignition at cold ambient cases. Thus, in order to investigate cold startability and cold idle behaviour, the institute VKA has performed optical investigations using a combustion vessel as well as an optically accessible diesel engine.

## 1 Introduction

New combustion systems show a significant progress in the improvement of exhaust raw emissions. In this respect, partly homogenous combustion processes are especially promising. To generate longer ignition delays, which are necessary for the homogenisation of the mixture, partly homogeneous systems require reduced compression ratios. Due to the lower compression temperature and pressure, however, both evaporation and ignition of the fuel are impeded, especially at very low ambient temperatures [1, 2, 3, 4]. Consequently the start-up behaviour is deteriorated and white smoke emissions are increased. In view of customer requirements and impending emissions regulations, both effects have to be taken into account [5, 6, 7, 8].

In **Figure 1**, the engine speed curves of two cold starts, performed at an ambient temperature of −27 °C, are displayed over time. The cold starts were performed using two engines with compression ratios of 18:1 and 16:1 respectively. The engine with the higher compression ratio reaches idle speed – after a small overshoot – within 7 s. With the reduced compression ratio of 16:1, however, the period from cranking to idle speed almost doubles. In addition, the engine speed fluctuations at cold idle are significantly higher as at a compression ratio 18:1, which is a result of the higher variance in indicated mean effective pressure.

## 2 Method of Investigation

For the cold start investigations, both a high pressure vessel and a single-cylinder optical diesel engine were used. The high pressure chamber is fed by a continuous air flow with a maximum pressure of 6 MPa and a maximum temperature of 550 °C. The cold start measurement equipment was implemented using a special chamber adapter equipped with a cooling channel, a rotatable injector mounting device and a glow plug bore. For the visualisation of the spray penetration and the combustion process, shadow-graph and Schlieren techniques in combination with high-speed video imaging were being used. The basic of Schlieren technique is as follows: parallel light passing through the test medium are shadowed by the liquid fuel or are deflected by the flow density gradients of the gaseous fuel. Dark areas on the photographic image can be attributed to liquid fuel, while gaseous fuel is indicated by the typical Schlieren patterns.

VKA's optical single-cylinder diesel engine is based on a production engine with a total displacement of 1.9 l. An intermediate construction between the modified cylinder head and the cylinder block facilitates the operation of an elongated piston with a quartz glass piston bowl. The remaining three cylinders are inoperative. As illustrated in **Figure 2**, by means of a mirror, the processes within the combustion chamber can be recorded with a digital high-speed camera.

### 2.1 Application of the Cooling Devices

The cooling power required for the experiments in both the combustion chamber and in the optical single-cylinder diesel engine was provided by a cooling unit, see No. 11 in **Figure 3**. In addition, for the cooling process, a dehumidifier was required to collect the condensed water. A schematic diagram of the complete cooling circuit for the optical diesel single-cylinder engine is displayed in Figure 3. From the cooling unit and the cooling tank, two circuits, each fed by means of a circulation pump, provided

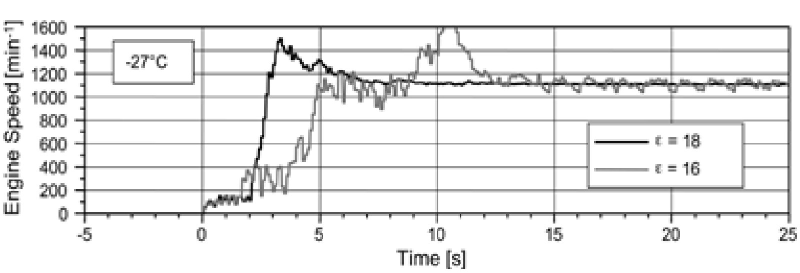


**Figure 1:** Cold-starting with different compression ratios

## Authors

Prof. Dr.-Ing. Stefan Pischinger is head of Lehrstuhl für Verbrennungskraftmaschinen (VKA) of the RWTH Aachen (Germany).

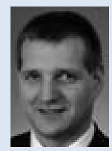

Dipl.-Ing. Ulrich Grütering is commercial manager of Lehrstuhl für Verbrennungskraftmaschinen (VKA) of the RWTH Aachen (Germany).

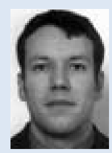

Dipl.-Ing. Markus Graf was until end of September 2007 scientific assistant at the Lehrstuhl für Verbrennungskraftmaschinen (VKA) of the RWTH Aachen (Germany).

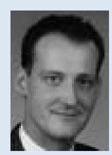

Priv.-Doz. Dr.-Ing. Philipp Adomeit is general manager Innovation Thermodynamics at the FEV Motorentechnik GmbH in Aachen (Germany).

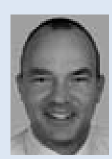

Dipl.-Ing. Lothar Schmid was head of the FVV working group and is team manager passenger cars diesel combustion processes in the R&D department of the Daimler AG in Stuttgart (Germany).

the test bench with the required coolant (No. 2 and No. 7). One coolant circuit supplied coolant to a utility vehicle intercooler (No. 14), to an intercooler for the charging device (No. 15), and to a precooling device (No. 16). The other circuit supplied coolant to the cylinder head and the water jacket of the liner (No. 3). Also connected to this circuit were the fuel tank (No. 1) and the fuel rail (No. 6). In order to attain the required temperature of −20 °C, a third intercooler was positioned immediately upstream of the intake manifold (No. 10). For experiments conducted at low engine speeds, a planetary gearbox was installed (No. 12).

For the cold start experiments using the combustion vessel, the chamber adapter, the fuel rail as well as the fuel tank were connected to the cooling unit. The coolant was supplied by means of one of the circulation pumps used for the optical engine test bench.

## 2.2 Application of the Glow Plugs

For the research project, steel glow plugs with integrated thermo couples were provided by Beru, which made possible to measure the glow temperatures during the test. In the course of the investigations, these glow plug temperature measurements turned out to be essential, since the heat transfer was affected by the varying air-flow conditions, and that the glow plug voltages had to be adjusted to compensate this effect.

**Figure 4** shows the voltage as well as the current and temperature curves of a steel glow plug with an integrated type-K thermocouple (Ni-Cr-Ni) over a period of 30 s. First, the instant start system supplies a boost voltage of 11 V. After 1.9 s, the quick-start plug [5] reaches its end temperature of 1100 °C at the surface. After this 1.9 s, the voltage is reduced to 4.4 V. The surface temperature of the glow plug peak is not uniform. There is a hot spot whose temperature is higher than that of the surrounding glow plug surface.

Apart from the steel glow plug measurements, further investigations were conducted using a production ceramic glow plug. However, in operation with the specific nominal voltage the required stationary nominal temperature could not be achieved. Therefore, the

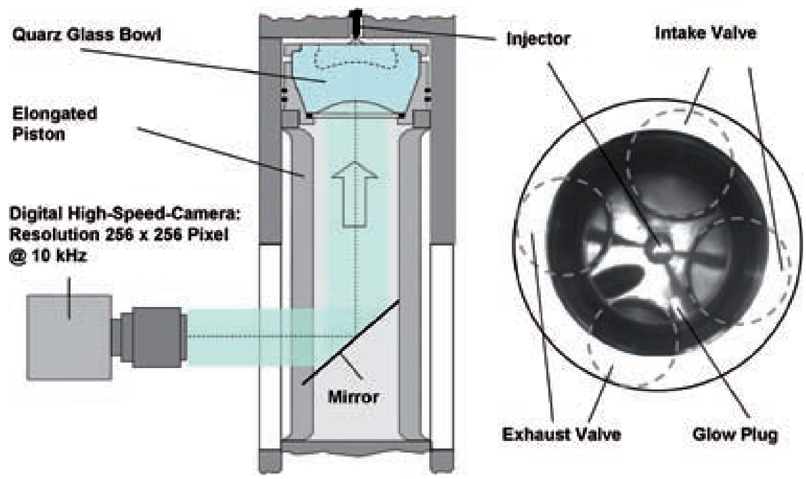


**Figure 2:** Setup of the single-cylinder diesel engine for the optical measurements

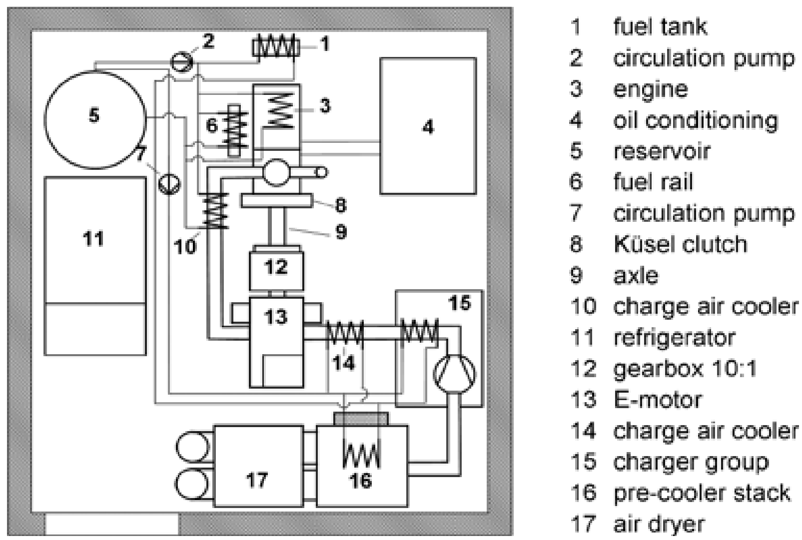


**Figure 3:** Cooling circuits in the test bench of the optical single-cylinder diesel engine

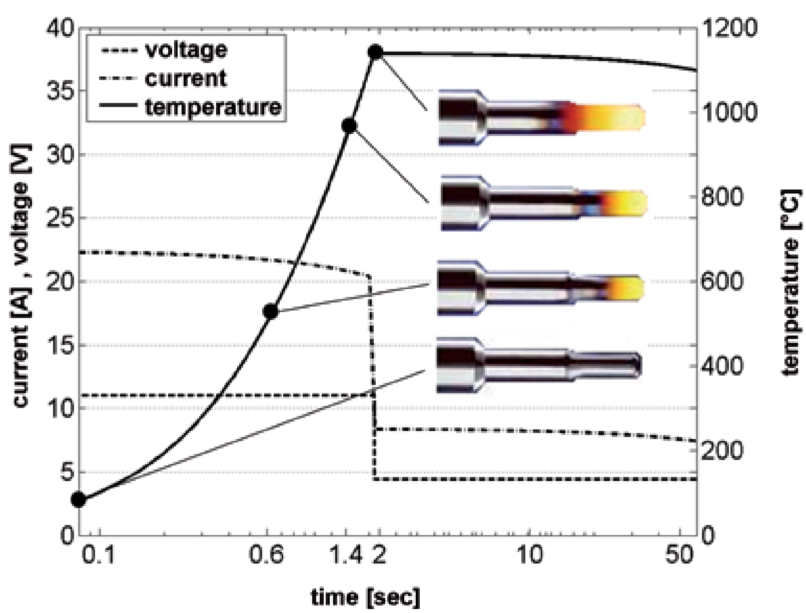


**Figure 4:** Traces for current, voltage and temperature of a steel glow plug [5]

results of the investigations using the ceramics glow plug were not further considered.

## 2.3 Measurement Programme

In close coordination with the FVV working group, the variation parameters, displayed in the table of **Figure 5**, were decided. The dimensions and angles, presented in Figure 5, can be comprehended with the chamber adapter scheme.

Within the high pressure combustion chamber, the gas pressures and temperatures can be adjusted independently of each other. The engine‘s end compression pressure and end compression temperature, however, are coupled with the intake manifold density, the compression ratio, as well as the wall heat transfer and blow-by losses. For the investigations using the optical single-cylinder diesel engine, the focus lay on the variation of three parameters: the engine speed n, the rotating angle of the injector $\alpha_{GK}$ and the glow plug protrusion $d_{GK}$ were varied.

| Gas | Injection / Fuel | Glow Plug |
|---|---|---|
| • pressure | • temperature | • type |
| • temperature | • actuation duration | • distance $r_{GK}$ |
| • engine speed | • fuel type | • angle $\alpha_{GK}$ |
| | • strategy | • protrusion $d_{GK}$ |
| | • rail pressure | • temperature |

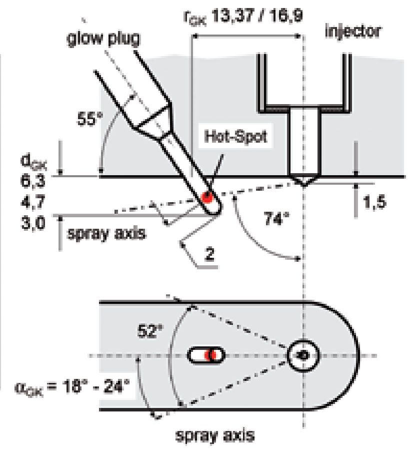


**Figure 5:** Variation parameters displayed in the table and geometric measurements

Depending on the experimental boundary conditions only parts of the mixture or the entire area of ignitable, vaporised fuel are incorporated in the reaction zone. To complement the visualisation of the injection process, a progress bar of the needle lift signal is displayed below the frame.

The results of the high-speed imaging investigations focus on the evaluation of the spray geometry and the reaction zone of the left-hand spray jet. The dimension of the reaction zone is indicated by the total sum of overexposed pixels. **Figure 7** shows the mean values of the normalised needle lift signal over time, beginning with the start of injection. The corresponding mean value of the size of the flame surface is displayed in a logarithmic scale. The error bars of both the needle lift signal and flame area show the absolute minimum and maximum obtained in ten repetitive measurements under steady boundary conditions.

## 3 Results

In the following results for combustion vessel and optical engine but also a phenomenological description of the glow plug assisted combustion are presented.

## 3.1 Combustion Vessel

**Figure 6** shows a recorded sequence of frames from the high-speed camera of an injection process with glow plug-assisted combustion. The images taken within the first millisecond are not displayed, as the cold injector containing the cold fuel opens very slowly. After one millisecond, until approximately 3.7 ms, every tenth video frame is being displayed. After that, until approximately t = 4.7 ms, every fifth frame is being shown.

At the time 3 ms after the start of injection, a reaction zone is visible for the first time, as seen in Figure 6. In the different experiments, the time of the onset of the first reaction varied. Furthermore the dimension of the reaction zone – which dwells at the glow plug until the injection needle closes – varied as well. Once no further high momentum fuel impinges on the glow plug, the reaction zone grows with cyclic fluctuations of flame propagation velocity.

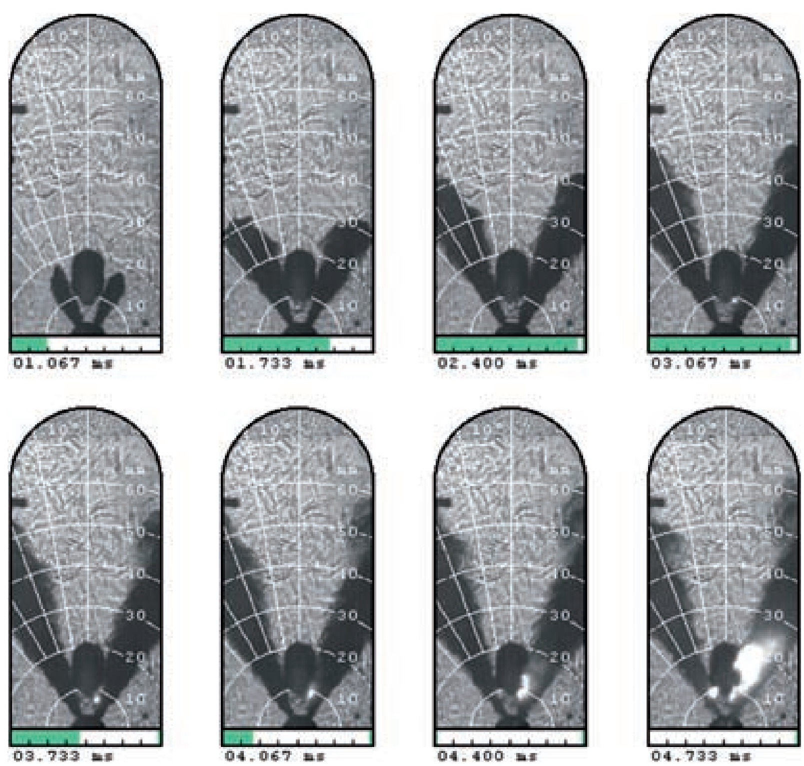


**Figure 6:** Exemplarily combustion vessel measurement

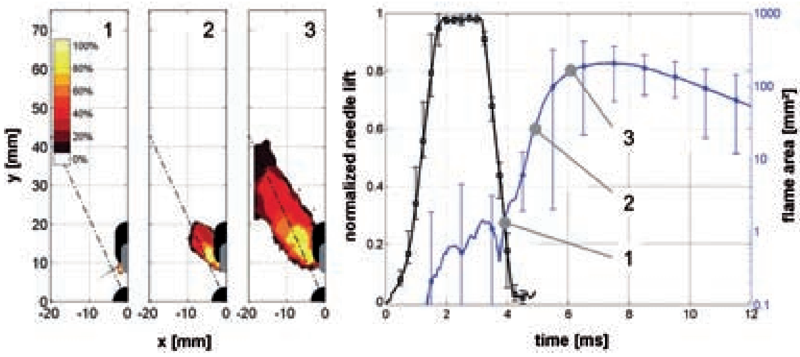


**Figure 7:** Evaluation of the results from the combustion vessel measurements – local defined flame probability (left) and flame surface and needle lift (right)

be calculated to describe the combustion during the cold start and cold idle operation. For comparison, in **Figure 9** are presented the measured heat release rates and the light intensities for a measurement point at engine speeds of 500 and 1000 rpm.

At the speed n = 500 rpm it is seen, that the combustion process begins while the nozzle needle is opening, and the level of the heat release rate remains constant at maximum needle lift. When the needle is closing, the heat release rate decreases shortly, but rises again after the injection process is completed. Subsequently it reaches its maximum and then decreases in the course of the expansion stroke. Furthermore, it can be seen that the interim drop of heat release is most prominent when the fuel directly impinges on the glow plug. It is also of interest that in case of a large distance between the spray cone boundary and the glow plug surface, the drop in heat release rate does not immediately follow the needle lift signal, but with a certain delay. Comparing the light intensity curve with the heat release curve, it becomes apparent that there is no visible soot luminescence during the first phase of the combustion, during the injection process. The soot luminescence occurs for the first time during the process of needle closing.

The heat release curve at 1000 rpm differs from the heat release curve at 500 rpm. At first sight, there is no direct

To investigate the effect of parameter variations on the combustion process, three characteristics were calculated:

1. The flame area A, averaged over time
2. The time $t_{50\%}$ needed for the flame surface to attain half of its maximum value
3. The variance σ of the flame propagation.

With increasing injection duration and larger injected fuel quantities, the flame area strongly expands. On the one hand, low fuel quantities burn faster, on the other hand, with low fuel quantities, the relative standard deviation increases. With higher gas temperatures, both the size of the reaction zone and the flame propagation velocity increases. At the same time, the mean standard deviation decreases. An analogous dependency is observed when the fuel temperature and the rail pressure are varied. While the effect of the gas and fuel temperature can be explained by the faster evaporation process due to increasing temperatures, the improved combustion at higher rail pressures is a result of the increased entrainment of hot air from the glow plug boundary layer into the spray.

Apart from these parameter variations discussed above, the influence of different fuels and injection strategies as well as of different protrusions and glow plug temperatures were examined. With larger protrusion and higher glow plug temperature, ignition and combustion improve. In the combustion chamber, split injection did not show any noticeable advantage compared to single injection. The differences between arctic fuel and winter diesel proved to be insignificant, so that in the further course of the investigations only arctic fuel was used, as it has a lower cold plugging point. N-heptane has a boiling point of 98 °C, which lies significantly below the evaporation curves of artic fuel and winter diesel. Therefore, at equal gas temperatures, the combustion of n-heptane is much faster, and the soot production is lower. The smaller soot quantity reduces the soot luminescence and directly affects the flame imaging results. Therefore, a direct comparison of n-heptane and diesel fuels is not possible.

## 3.2 Optical Engine

**Figure 8** shows the six adapted records of a high-speed video at a measurement point of n = 1000 rpm. Besides optical measurement results at the optical engine, data of the pressure indication can

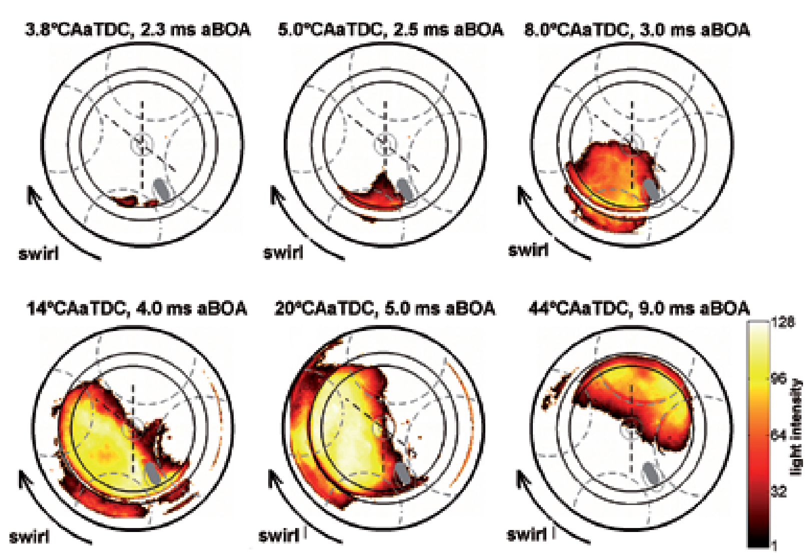


**Figure 8:** Exemplarily measurement at the optical engine

relation between the needle lift signal and the heat release curve at the higher engine speed, which is due to the longer ignition delays. Obviously, at this engine speed, the combustion process is not primarily determined by the fuel spray, but by the turbulent swirl flow. In case that the fuel directly impinges on the glow plug, once more, the characteristic drop in heat release rate can be witnessed once the injection process is completed. A correlation between the ignition delays and the durations until the first occurrence of soot luminescence for the three injector angle variations demonstrates that there is a linear relationship between the curve of the light intensity and the curve of the heat release rate.

### 3.3 Phenomenological Description of the Glow Plug Assisted Combustion

Based on the visualisation results within the combustion vessel and the optical engine, the following summarising statements can be made: A reliable direct ignition of the fuel during cold start requires to carefully adjust the fuel spray relative the glow plug. If the fuel impinges on the glow plug, then ignition takes place even at low glow plug temperatures. For engine application purposes, however, this case is of less importance. If the injector is rotated to maintain no contact between fuel and the glow plug, an optimal position is achieved to get a maximum indicated mean effective pressure with acceptable cycle-to-cycle fluctuations.

A typical glow plug induced ignition is shown in **Figure 10** as a sequence of images of ignition and flame propagation. It is seen, that the flame kernel develops in a limited volume in the vicinity of the glow plug surface. The subsequent flame growth occurs with a noticeable delay. In the following a phenomenological approach is presented, which first describes the processes, and subsequently explains it by theoretical considerations.

The right part of Figure 10 shows the area between the nozzle tip and the glow plug. At the time of ignition, the injection spray in this area can be described by the theory of a turbulent free jet, as the injection process is stationary at this time (see Figure 7). The jet-induced flow field in the area between the injector and the glow plug can be calculated by superposition of the free jet flow field with a potential field around the glow plug [9]. In Figure 10, selected streamlines (black lines) of the flow field are depicted. The model parameters for calculation are adjusted to meet the spray tip velocity and the injection angle derived from the shadowgraph Schlieren imaging. Within the margins of the free jet (dash-pointed lines) the fuel steam distribution can be calculated according to Abramovich [10]. In Figure 10, the grey-coloured areas of the field of air/fuel ratio $r_{AFR}$ indicate air/fuel ratio values within the ignition boundaries for diesel fuel ($r_{AFR}$ = 0.48 to 1.35).

In the period between t = 3.4 ms after the start of injection and 4.6 ms after the start of injection, a circular reaction zone of intensive soot luminescence becomes visible, which remains at a fixed location close to the glow plug, and increases in diameter during time. The centre of the reaction zone is located on the direct connection line between the glow plug centre and the spray axis (shown as a dashed line in Figure 10). From 3.4 to 4.4 ms the increase of reaction zone diameter occurs proportional to the decrease in needle lift and thus also proportional to the decrease in mean velocities within the flow field.

At the end of the injection, at t = 4.6 ms, the flame propagates rapidly along the spray direction through regions with a near-stoichiometric air/fuel ratio. This results in a large extension of the reaction zone. Within this zone turbulent diffusive combustion predominates, as revealed by the intensive soot luminescence.

Overall, that means the ignition process consists of several phases with distinct dynamics. This can be illustrated by taking a close look at the time scales of the process. At the beginning and during the injection event, no visible combustion with soot luminescence can be observed, even with sufficiently high gas temperatures. The dwell time of the ignitable mixture in the reaction zone close to the glow plug is very short during this period. According to the Flamelet theory [11], this causes a high scalar dissipation rate, which inhibits reaction progress. During the needle-closing event the velocity along the spray axis and also in the reaction zone decreases rapidly. The scalar dissipation becomes smaller and a stationary, slowly growing reaction zone is formed, which is in a thermal equilibrium of reaction heat release heat losses due to convection. At the end of injection, the flow field collapses, and the scalar dissipation is reduced drastically. By this the condition for the flame propagation are altered, causing an explosive growth of the reaction zone by premixed combustion. The subsequent burn-out is dominated by diffusive combustion.

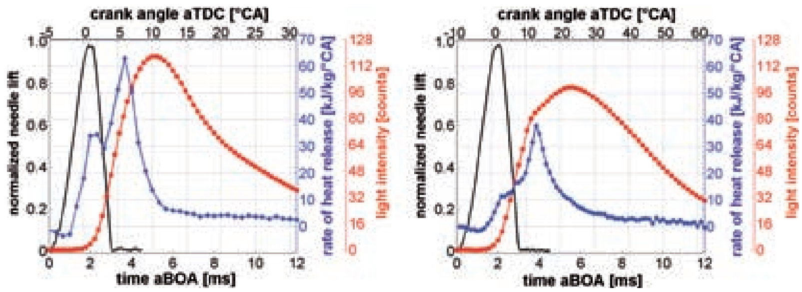


**Figure 9:** Evaluation of the results from the optical engine measurements (left: 500 rp, speed, right: 1000 rpm speed)

## 4 Summary

At the Institute for Combustion Engines of RWTH Aachen University, fundamental research on the glow-plug-assisted ignition of diesel fuel at low temperatures was conducted. For the investigations made in a FVV research project, a model combustion vessel and an optical diesel engine were being used. The measurements in the combustion chamber yielded information on the spray penetration as well as on the process of combustion.

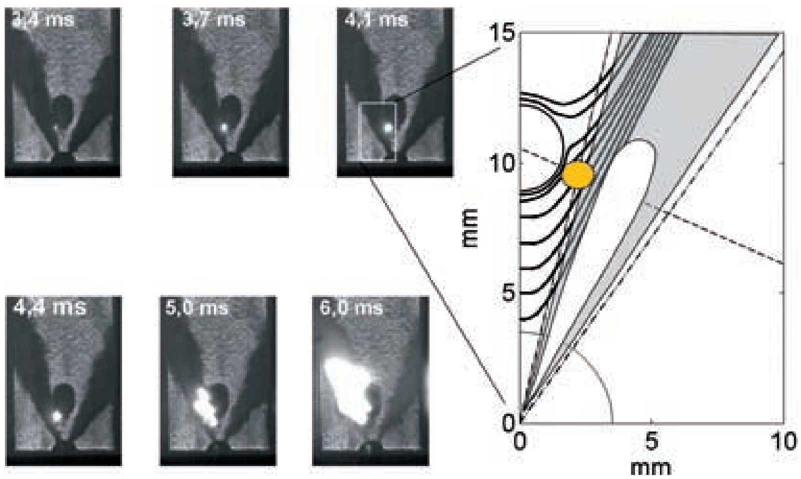


**Figure 10:** Interaction of the diesel injection spray with the glow plug

By analysing the soot luminescence at varying fuel quantity, it became apparent that small fuel quantities burn faster, but also show a distinctly larger spread/standard deviation than larger fuel quantities, a phenomenon hinting at ignition problems. Glow plug protrusions of $d_{GK}$ = 4.7 and 6.3 mm and adequate injector angles α in combination with a sufficiently long injection duration resulting in a large fuel quantity make it possible to inject the fuel tangentially onto the glow plug. As a result, a reaction zone at the glow plug is formed, which is liable to initiate the further combustion as soon as the injection process is completed.

For the interpretation of the results gained with the optical engine, the optical data of the high-speed imaging as well as the pressure curves can be used. The evaluation of the standard deviation σ of the indicated mean effective pressure (IMEP) demonstrates that the misfire probability increases with larger distances between the fuel jet and the glow plug as well as with smaller glow plug protrusions. Taking into account these conclusions in combination with the IMEP evaluation, an optimum glow plug / injector arrangement for cold idle operation can be arrived at. Correlating the results from the thermodynamic analysis with those of the corresponding optical combustion analysis, it can be demonstrated that there is no linear relationship between the mapping pairs under consideration, except in one case: At an engine speed of 1000 rpm, the beginning of the combustion process correlates with the beginning of the soot luminescence for all investigated parameter variations.

At an engine speed of 500 rpm, the curve of the heat release rate points to the fact that the combustion begins as early as during the injection process. This phase of the combustion process cannot be visualised by means of a standard high-speed camera, as it is sensitive for luminescence in the visible range only. It can be assumed that the combustion process in the pressure chamber begins before the first occurrence of visible soot luminescence.

Drawing on the theory of the free round turbulent jet, the location of the reaction zone with visible soot luminescence during the glow plug-assisted diesel ignition process can be qualitatively described. The simplified model, however, is not capable of a more detailed description, especially in case that jet-to-wall interactions play a major role, which is the case at high radial distances between the injector and the glow plug.

All investigations performed in the combustion chamber and in the optical engine have demonstrated that under cold start and cold idle conditions, any interaction between the fuel jet and the piston bowl is liable to result in a deterioration of the combustion process. The occurrence of swirl, in combination with decreasing blow-by and wall heat losses at increasing engine speeds, by contrast, is apt to stabilise the combustion.


### Acknowledgements

This contribution is the scientific result of the research project No. 862 “Dieselkaltlauf”, posed by the Research Association of Internal Combustion Engines e. V. (FVV) that was worked out at the Lehrstuhl für Verbrennungskraftmaschinen of the Rheinisch-Westfälische Technische Hochschule Aachen under the direction of Prof. Dr.-Ing. Stefan Pischinger. The work was financially promoted by FVV own resources. The project was accompanied by a working group of the FVV – first under the direction of the head Dipl.-Ing. Eberhard Holder and later of Dipl.-Ing. Lothar Schmid, both Daimler AG. The acknowledgement of the authors for the large support are entitled to this working group, in particular Robert Bosch GmbH for the supply of the injection system, the Beru AG for the supply of the measuring glow plugs as well as both the MAN AG and the Adam Opel AG for the free supply of materials.


## References


[1] Blanc, M.; Geiger, S.; Houben, H.; Hovestadt, T.; Toedter, O.: Diesel-Kaltstartsystem ISS der zweiten Generation mit Ansaugluft-Vorwärmung. In: MTZ 65 (2006), Nr. 5, S. 352–359

[2] Lin, H.; Henein, N. A.; Bryzik, W.: Simulation of Diesel-Engines Cold-Start. In: SAE 2003-01-0080 (2003)

[3] Han, Z.; Henein, N. A.; Bryzik, W.: Diesel Engine Cold Start Combustion Instability and Control Strategy. In: SAE 2001-01-1237 (2001)

[4] Zahdeh, A.; Henein, N. A.; Bryzik, W.: Diesel Cold Starting: Actual Cycle Analysis Under Border-line Conditions. In: SAE 900441 (1990)

[5] Houben, H.; Uhl, G.; Schmitz, H.-G.; Endler, M.: Das elektronisch gesteuerte Glühsystem ISS für Dieselmotoren. In: MTZ 61 (2000), Nr. 10, S. 668–675

[6] Kern, C.; Dressler, W.; Lindemann, G.; Rothacker, V.: An Innovative Glow System for Modern Diesel Engines. In: SAE 1999-01-1240 (1999)

[7] Osuka, I.; Nishimura, M.; Tanaka, Y.; Miyaki, M.: Benefits of New Fuel Injection System Technology on Cold Startability of Diesel. In: SAE 940586 (1994)

[8] Naber, D.; Dohle, U.; Krüger, M.; Schuhmacher, H.; Hondros, Ch.: Kaltstart und Kaltlaufuntersuchungen an direkt einspritzenden Pkw-Dieselmotoren. In: 15. Aachener Kolloquium Fahrzeug- und Motorentechnik (2006), S. 315–334

[9] Pope, S. B.: Turbulent Flows. Cambridge University Press, 1st Edition, New York (USA), 2000

[10] Abramovich, G. N.: The Theory of Turbulent Jets. M. I. T. Press, Cambridge, Mass. (USA), 1963

[11] Peters, N.: Turbulent Combustion. Cambridge University Press, 1st Edition, New York (USA), 2000

# Communicating in international business


Robert Bosch GmbH (Editor)

**Fachwörterbuch Kraftfahrzeugtechnik:**

Autoelektrik, Autoelektronik, Motor-Management, Fahrsicherheitssysteme

*German, English, French, Spanish*

3rd, fully revised and expanded edition 2005. 779 p.

€ 49.90 ISBN 3-528-23874-7

## THE CONTENT

Over 7600 specialist automotive engineering terms in English, French and Spanish translation, respectively sorted by one language as the source language with the remaining languages as target languages.

## THE BOOK

Based on the terminology contained in the individual Bosch reference books and the Automotive Handbook (Kraftfahrtechnisches Taschenbuch) as well as various other publications and glossaries, the motorcar specialist is provided with a compilation of the latest expert vocabulary in the languages German, English, French and now also Spanish. Essential for anyone wishing to remain capable of communicating in international business and hence constantly requiring the correct translation, even for new products and systems

## THE PUBLISHER

Robert Bosch GmbH is the world's largest motorcar outfitter. Bosch innovations have shaped the development of the modern automobile. The company's technological leadership in various areas is evidenced by the largest number of patent applications relating to automotive engineering in Germany, with the European patent office and in the USA.

## ORDER FORM

Yes, I hereby order:

___ Robert Bosch GmbH (Editor)
**Fachwörterbuch Kraftfahrzeugtechnik:**
Autoelektrik, Autoelektronik, Motor-Management, Fahrsicherheitssysteme
3rd edition 2005. € **49.90** (plus postage)
ISBN 3-528-23874-7

First Name/Name

Company Department

Street

City/Postal Code

Date, Signature

vieweg
Abraham-Lincoln-Straße 46
D-65189 Wiesbaden
Germany
Fax 0049.611.7878-420
www.vieweg.de

Prices and other details are subject to change without notice.

managing directors: Andreas Kösters,
AG Wiesbaden HRB 9754